

Lake Baikal isotope records of Holocene Central Asian precipitation

1
2

3 George E. A. Swann^{1,*}, Anson W. Mackay², Elena Vologina³, Matthew D. Jones¹, Virginia N. Panizzo¹, Melanie
4 J. Leng^{4,5}, Hilary J. Sloane⁴, Andrea M. Snelling¹, Michael Sturm⁶

5

6 ¹*School of Geography, Centre for Environmental Geochemistry, University of Nottingham, University Park,*
7 *Nottingham, NG7 2RD, UK*

8 ²*Environmental Change Research Centre, Department of Geography, UCL, London, UK*

9 ³*Institute of Earth's Crust, Siberian Branch of the Russian Academy of Sciences, Irkutsk, Russia*

10 ⁴*NERC Isotope Geosciences Facilities, British Geological Survey, Nottingham, NG12 5GG, UK*

11 ⁵*Centre for Environmental Geochemistry, School of Biosciences, Sutton Bonington Campus, University of*
12 *Nottingham, Loughborough, LE12 5RD, UK.*

13 ⁶*Eawag-ETH, Swiss Federal Institute of Aquatic Science and Technology, 8600, Dübendorf, Switzerland*

14

15 * *corresponding author george.swann@nottingham.ac.uk*

16

17 **Keywords:** Diatom; Mongolia; Paleoclimatology; Paleolimnology; Russia

18

19 **Abstract**

20 Climate models currently provide conflicting predictions of future climate change across Central Asia. With
21 concern over the potential for a change in water availability to impact communities and ecosystems across the
22 region, an understanding of historical trends in precipitation is required to aid model development and assess
23 the vulnerability of the region to future changes in the hydroclimate. Here we present a record from Lake
24 Baikal, located in the southern Siberian region of central Asia close to the Mongolian border, which
25 demonstrates a relationship between the oxygen isotope composition of diatom silica ($\delta^{18}\text{O}_{\text{diatom}}$) and
26 precipitation to the region over the 20th and 21st Century. From this, we suggest that annual rates of precipitation
27 in recent times are at their lowest for the past 10,000 years and identify significant long-term variations in
28 precipitation throughout the early to late Holocene interval. Based on comparisons to other regional records,
29 these trends are suggested to reflect conditions across the wider Central Asian region around Lake Baikal and
30 highlight the potential for further changes in precipitation with future climate change.

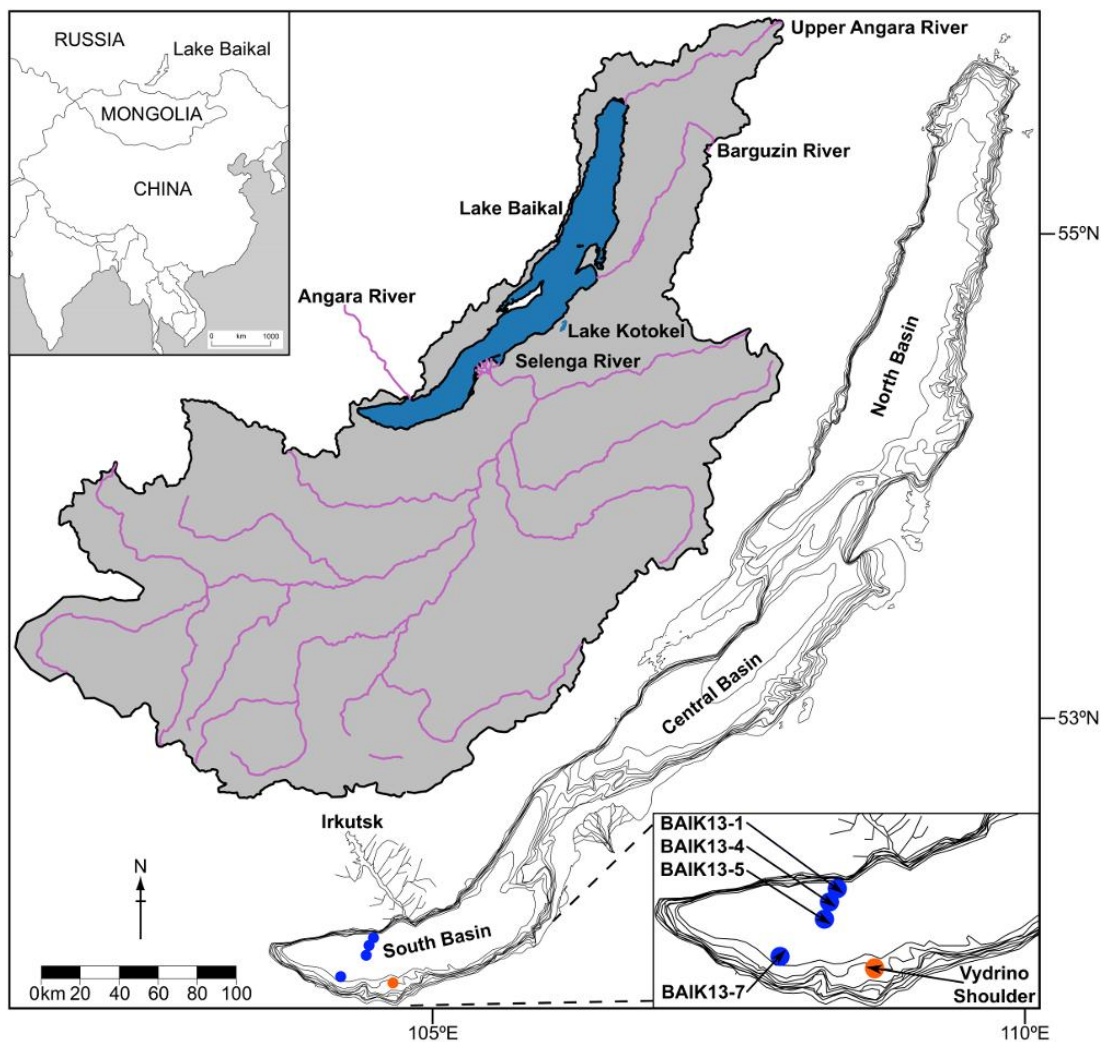
31 1 Introduction

32 The forest-steppe ecotone of Central Asia is dominated by grassland and taiga ecosystems that are vulnerable to
33 both changes in the climate and other anthropogenic activities (Craine et al., 2012; Hijioaka et al., 2014; Settele
34 et al., 2014; Tautenhahn et al., 2016). Declines in precipitation over the past three decades have led to marked
35 reductions in grassland biomass across the Mongolian steppes and wider region (Endo et al., 2006; Liu et al.,
36 2013; Li et al., 2015), whilst global reductions in boreal forest due to fire and forestry are second only to losses
37 in tropical forests (Hansen et al., 2013). Ongoing work points to the continuing fragility of these ecosystems.
38 For example, 21st Century climate change across Central Asia is likely to lead to a northward migration of the
39 forest-steppe ecotone with remaining forest stand height highly dependent on rates of precipitation
40 (Tchebakova et al., 2009; 2016). At the same time reductions in soil moisture associated with climate change
41 are expected to accelerated grassland degradation, negatively impacting nomadic pastoralism (Liu et al., 2013;
42 Sugita et al., 2015), whilst issues of water security are likely to be exacerbated by plans for increased
43 groundwater extraction and dam construction (Karthé et al., 2015). Growth of hemi-boreal forests in the forest -
44 steppe ecotone has already slowed, linked to decline soil water content due to regional warming (Wu et al.
45 2012).

46
47 Changes in the central Asian hydrological cycle will also alter regional carbon cycling. The increased risk of
48 fires across grasslands and boreal forest will impact vegetation regeneration (Tchebakova, 2009; IPCC, 2012;
49 Tautenhahn et al., 2016) and lead to an immediate increase in atmospheric CO₂ (Randerson et al., 2006).
50 Reductions in soil moisture availability and rising temperatures will further reduce carbon terrestrial storage by
51 increasing the decomposition of organic matter in soils and lowering net carbon uptake by plants (Lu et al.,
52 2009; Crowther et al., 2016). However, more significant are the threats posed by permafrost degradation,
53 particular in southern Siberia and northern Mongolia where permafrost is vulnerable to degradation through
54 warming, human impacts and increased wildfires (Sharkuu, 1998; Romanovsky et al., 2010; Zhao et al., 2010;
55 Törnqvist et al., 2014). Combined, these processes will release carbon to the atmosphere (Schuur et al., 2015)
56 and increase organic carbon export to water bodies (Selvam et al., 2017).

57
58 In order to improve future predictions of the Central Asian hydrological cycle there is an urgent need to
59 understand long-term changes in the climate system beyond the instrumental record. Here we use the oxygen
60 isotope composition of diatom silica ($\delta^{18}\text{O}_{\text{diatom}}$) from Lake Baikal (Russia) to constrain historical changes in

61 Central Asian precipitation over the last 10,000 years, within the context of the modern day. Situated at the
 62 edge of the forest-steppe ecotone, the lake's catchment extends into northern Mongolia (Fig. 1) and is highly
 63 sensitive to changes in the hydrological cycle. Future changes in the region have the potential to reduce river
 64 flow around Lake Baikal, impacting the provision of water to one of the world's greatest lakes (Törnqvist et al.,
 65 2014) as well as decreasing soil moisture content and so increasing the risk of forest fires and associated carbon
 66 release (Forkel et al., 2012). Concurrently, climate change is likely to lead to further loss of permafrost across
 67 the region (Sharkuu, 1998; Törnqvist et al., 2014), potentially increasing the flow of dissolved organic carbon
 68 into Lake Baikal (Mackay et al., 2017) and altering the microbial food web, nutrient recycling and carbon
 69 processing within this ecological sensitive lake (Moore et al., 2009).



70 Figure 1: Location of Lake Baikal and its catchment (grey region) together with Lake Kotokel, the city of
 71 Irkutsk, major rivers, coring sites BAIK13-1, BAIK13-4, BAIK13-5, BAIK13-7 (blue circles) and Vydrino
 72 Shoulder (orange circle).

73 **1.1 Lake Baikal reconstructions of the hydrological cycle**

74 Lake Baikal is the world's oldest, deepest and most voluminous lake and, located in southern Siberia, contains
 75 c. 20% of the world's surface freshwater not stored within ice. The lake is divided into three basins (south,
 76 central and north) separated by the Buguldeika Saddle and the Academician Ridge, respectively (Fig. 1). Inputs
 77 of water to the lake are primarily derived from direct precipitation (c. 16%) and riverine inputs (c. 80%) (Seal
 78 and Shanks, 1998). Groundwater inputs are minor, believed to provide <4% of annual inflow (Seal and Shanks,
 79 1998), although no systematic study has been carried out on groundwater, its residence time or isotope
 80 composition. Whilst over 350 rivers drain an area of c. 540,000 km² into Lake Baikal, inputs are dominated by
 81 the Selenga River, extending south into Mongolia, and the Upper Angara and Barguzin Rivers, draining the
 82 north of the catchment, which contribute c. 62%, 17% and 8% of riverine input respectively (Seal and Shanks,
 83 1998) (Fig. 1).

84
 85 Once in Lake Baikal, surface waters that extend down to the mesothermal maximum (MTM) at a depth of 200-
 86 300 m undergo convective mixing (Shimaraev et al., 1994; Shimaraev and Domysheva, 2004) and wind forced
 87 convection (Troitskaya et al., 2015). Whilst deeper waters are stratified (Shimaraev and Granin, 1991;
 88 Shimaraev et al., 1994; Ravens et al., 2000), they are exchanged across the MTM through periodic upwelling
 89 and downwelling episodes (Weiss et al., 1991; Shimaraev et al., 1993, 1994, 2012; Kipfer et al., 1996;
 90 Hohmann et al., 1997). Finally, water loss from Lake Baikal is dominated by outflow through the Angara River
 91 in the south basin of Lake Baikal (c. 79%) and evaporation (c. 19%), with an additional unconstrained loss
 92 from groundwater estimated at <2% of total outflow (Seal and Shanks, 1998; Shimaraev et al., 1994).

93
 94 Over the past 15 years, significant effort has been devoted towards developing and applying $\delta^{18}\text{O}_{\text{diatom}}$ in
 95 palaeoenvironmental reconstructions due to its ability to reflect the isotope composition of ambient water
 96 ($\delta^{18}\text{O}_{\text{water}}$). With the controls on $\delta^{18}\text{O}_{\text{diatom}}$ similar to those for carbonates, $\delta^{18}\text{O}_{\text{diatom}}$ represents an important source
 97 of information in aquatic ecosystems such as Lake Baikal where carbonates are poorly preserved (Leng and
 98 Barker, 2006). In Lake Baikal, mixing of the water column leads to uniform surface and deep $\delta^{18}\text{O}_{\text{water}}$ of -15.8
 99 $\pm 0.2\text{‰}$, whilst riverine inputs ($\delta^{18}\text{O}_{\text{river}}$) vary latitudinally from -13.4‰ to -21.2‰ in relation to the
 100 isotopically low winter precipitation in the north ($\delta^{18}\text{O}_p$) and higher summer $\delta^{18}\text{O}_p$ in the south (Seal and
 101 Shanks, 1998; Morley et al., 2005). With riverine inputs accounting for c. 80% of all inflow to the lake, spatial
 102 and temporal changes in $\delta^{18}\text{O}_p$ across the catchment have been proposed to change both $\delta^{18}\text{O}_{\text{river}}$ and the relative

103 balance of north versus south basin river discharge to the lake, processes that in turn alter $\delta^{18}\text{O}_{\text{water}}$ (Morley et
104 al., 2005). On this basis, records of $\delta^{18}\text{O}_{\text{diatom}}$ can be used to monitor these changes in the regional Central Asian
105 hydroclimate.

106

107 To date, this interpretation has been applied to interglacial records from Lake Baikal spanning the Holocene,
108 MIS 5e and MIS 11 to constrain temporal variations in the penetration of westerlies into Central Asia and
109 regional atmospheric circulation involving the Siberian High (Mackay et al., 2008, 2011, 2013). However, no
110 empirical relationship has been demonstrated between hydroclimate variability and down-core records of
111 $\delta^{18}\text{O}_{\text{diatom}}$. The absence of such a calibration prevents: 1) a full quantitative interpretation of the $\delta^{18}\text{O}_{\text{diatom}}$ data
112 from Lake Baikal; 2) the integration of hydroclimate information in data-model comparisons to validate climate
113 model outputs (e.g., Haywood et al., 2016; PAGES Hydro2k Consortium, 2017); and 3) insight of how the
114 regional Central Asian climate behaved in intervals which might represent a future climate state. Here we
115 consider point #1 through the presentation of new $\delta^{18}\text{O}_{\text{diatom}}$ data from a series of cores from the south basin of
116 Lake Baikal that are compared to meteorological data over the last century and then employed to constrain
117 historical changes in Central Asian precipitation through the Holocene. In demonstrating a relationship between
118 $\delta^{18}\text{O}_{\text{diatom}}$ and precipitation, we highlight that levels of precipitation are today at their lowest levels for the last
119 10,000 years (10 ka), indicating the vulnerability of the region to future changes in precipitation and its
120 associated impact on ecosystem disturbance and terrestrial carbon cycling.

121

122 **2 Method**

123 **2.1 Sediment coring**

124 Four short sediment cores were collected from the south basin of Lake Baikal in March and August 2013 using
125 a UWITEC corer with PVC-liners (\varnothing 63 mm) which provided complete and undisturbed recovery of the highly
126 susceptible sediment/water interface of the cores (Fig. 1). Multiple cores were collected from each of the sites
127 in March 2013 through c. 78–90 cm of ice: BAIK13-1 ($51^{\circ}46'04.2''\text{N}$, $104^{\circ}24'58.6''\text{E}$, water depth = 1,360 m),
128 BAIK13-4 ($51^{\circ}41'33.8''\text{N}$, $104^{\circ}18'00.1''\text{E}$, water depth = 1,360 m) and BAIK13-5 ($51^{\circ}39'01.9''\text{N}$,
129 $104^{\circ}16'26.8''\text{E}$, water depth = 1,350 m). Further cores were then collected from BAIK13-7 ($51^{\circ}34'06''\text{N}$,
130 $104^{\circ}31'43''\text{E}$, water depth = 1,080 m) in August 2013 aboard the Geolog research boat from the Institute of the
131 Earth's Crust/Irkutsk (Fig. 1). At each site cores were labelled alphabetically with one core from each site
132 (BAIK13-1C [50 cm], BAIK13-4F [33 cm], BAIK13-5C [42 cm], BAIK13-7A [47.5 cm]) sub-sampled in the

133 field at a resolution of 0.2 cm and transported to the UK for $\delta^{18}\text{O}_{\text{diatom}}$ analysis. Parallel cores (BAIK13-1A [49.3
134 cm], BAIK13-4C [38.3 cm], BAIK13-5A [43.4 cm], BAIK13-7B [47.2 cm]) were transferred to the Institute of
135 the Earth's Crust/Irkutsk before being cut, photographed and lithologically described, based on smear slide
136 inspection. A Bartington MS2E High Resolution Surface Scanning Sensor (Bartington, 1995) was used for non-
137 destructive measurement of magnetic susceptibility (MS), with a resolution of 1 cm and reproducibility of <5%.

138

139 **2.2 Age models**

140 Dried samples from BAIK13-1C, BAIK13-4F and BAIK13-7A were analysed for ^{210}Pb , ^{137}Cs and ^{241}Am by
141 direct gamma assay in the Environmental Radiometric Facility at University College London, using ORTEC
142 HPGe GWL series well-type coaxial low background intrinsic germanium detector. No dating was carried out
143 on core BAIK13-5C. Instead, results from BAIK13-5C are included for the purpose of qualitative comparisons
144 with $\delta^{18}\text{O}_{\text{diatom}}$ data from other sites. ^{210}Pb was determined via its gamma emissions at 46.5 keV following
145 storage for three weeks in sealed containers to allow radioactive equilibration. ^{137}Cs and ^{241}Am were measured
146 by their emissions at 662 keV and 59.5 keV (Appleby et al, 1986). Corrections were made for the effect of self-
147 absorption of low energy gamma rays within the sample (Appleby et al, 1992), with the absolute efficiencies of
148 the detector determined using calibrated sources and sediment samples of known activity. To construct the final
149 age-depth models a polynomial regression was fitted to the ^{210}Pb data with additional degrees added until no
150 further improvements occurred in the fitted age-depth model against the old age-depth model under an ANOVA
151 test at the 95% confidence interval.

152

153 **2.3 Diatom oxygen isotopes**

154 Thirty samples from cores BAIK13-1C, BAIK13-4F, BAIK13-5C, BAIK13-7A were prepared for diatom
155 isotope analysis (see Supplementary Table 1) following the methodology in Swann et al. (2013) in which a
156 combination of 5% HCl and 30% H_2O_2 are used alongside sodium polytungstate in heavy liquid separation at
157 specific gravities of c. 2.2 g/ml^{-1} to remove non-diatom contaminants. Prior to analyses all samples were
158 screened using a Zeiss Axiovert 40 C inverted microscope, scanning electron microscope (SEM) and X-ray
159 fluorescence (XRF) to confirm sample purity and the absence of non-diatom contaminants. Diatoms in the
160 analysed samples are dominated by mainly endemic species including *Aulacoseira baicalensis*, *Aulacoseira*
161 *skvortzowii*, *Crateriportula inconspicua*, *Cyclotella minuta*, *Stephanodiscus meyerii* and *Synedra acus* var.
162 *radians*. Given the functional ecology of taxa in the analysed samples, our isotope records are interpreted as

163 recording mean annual conditions with a small bias towards spring months when diatom productivity peaks
 164 shortly after ice break-up (Popovskaya, 2000). This is justified by the long residence time of water in the south
 165 basin (Shimaraev et al., 1994) and homogeneity in $\delta^{18}\text{O}_{\text{water}}$ across the modern lake (Seal and Shanks, 1998;
 166 Morley et al., 2005) which should lead to minimal intra-seasonal variations in both $\delta^{18}\text{O}_{\text{water}}$ and $\delta^{18}\text{O}_{\text{diatom}}$.

167

168 Samples were analyzed for $\delta^{18}\text{O}_{\text{diatom}}$ using a step-wise fluorination procedure at the NERC Isotope Geosciences
 169 Facility based at the British Geological Survey (Leng and Sloane, 2008). Isotope measurements were made on a
 170 Finnigan MAT 253 and converted to the Vienna Standard Mean Ocean Water (VSMOW) scale using the
 171 within-run laboratory diatom standard BFC_{mod} calibrated against NBS28. Where necessary, samples were
 172 corrected for oxygen bearing contaminants using a geochemical mass balance approach developed for Lake
 173 Baikal (Mackay et al., 2011). The issue of contaminants can be problematic in Lake Baikal due to
 174 aluminosilicates trapped within the cylindrical frustules of *Aulacoseira* species (Brewer et al., 2008). To
 175 account for this, contaminants were calculated using XRF Al_2O_3 concentrations following the mass-balance
 176 approach in Mackay et al. (2011) in which samples are corrected for an assumed diatom bound Al
 177 concentration of 0.3 wt%, and used to model contaminant oxygen using Lake Baikal end-members in which
 178 aluminosilicates contain 17.2% Al with a $\delta^{18}\text{O}$ composition of $11.7\text{‰} \pm 0.3\text{‰}$ (Brewer et al., 2008).

179

180 **2.4 Climatological data**

181 To assess the controls on $\delta^{18}\text{O}_{\text{diatom}}$, results were compared to climatological data from World Meteorological
 182 Organisation station 30710 (52°16'20" N, 104°18'29" E, elevation = 467 m), located in Irkutsk close to the south
 183 basin of Lake Baikal (Fig. 1) with data from 2016-1891 obtained via the KNMI Climate Explorer
 184 (<http://climexp.knmi.nl/>). For all statistical analyses, autocorrelation was checked for using a Durbin-Watson
 185 test. Unless specifically stated, datasets were not autocorrelated. Values of $\delta^{18}\text{O}_p$ were calculated following Seal
 186 and Shanks (1998) who established a relationship ($r^2 = 0.768$) between $\delta^{18}\text{O}_p$ and surface air temperature (SAT)
 187 of:

188

189

$$\delta^{18}\text{O}_p = 0.361 \cdot \text{SAT} - 16.798$$

190

(Eq. 1)

191 With >95% of water inputs to the lake originating from direct precipitation or riverine inputs (Seal and Shanks,
 192 1998), changes in monthly isotopic inputs to Lake Baikal can be obtained by multiplying $\delta^{18}\text{O}_p$ by the amount

193 of monthly precipitation to account for seasonal variations in precipitation. Monthly values can then be
 194 summed to calculate annual inputs with values normalised relative to results for 2016 (δ_{influx}):

$$\delta_{\text{influx}} = \left(\frac{\sum_{\text{January}}^{\text{December}} \delta^{18}\text{O}_p \cdot \text{Precipitation (mm/month}^{-1})}{\text{Days in year}} \right) / \delta_{2016\text{influx}}$$

195 (Eq. 2)

196

197 **3 Results**

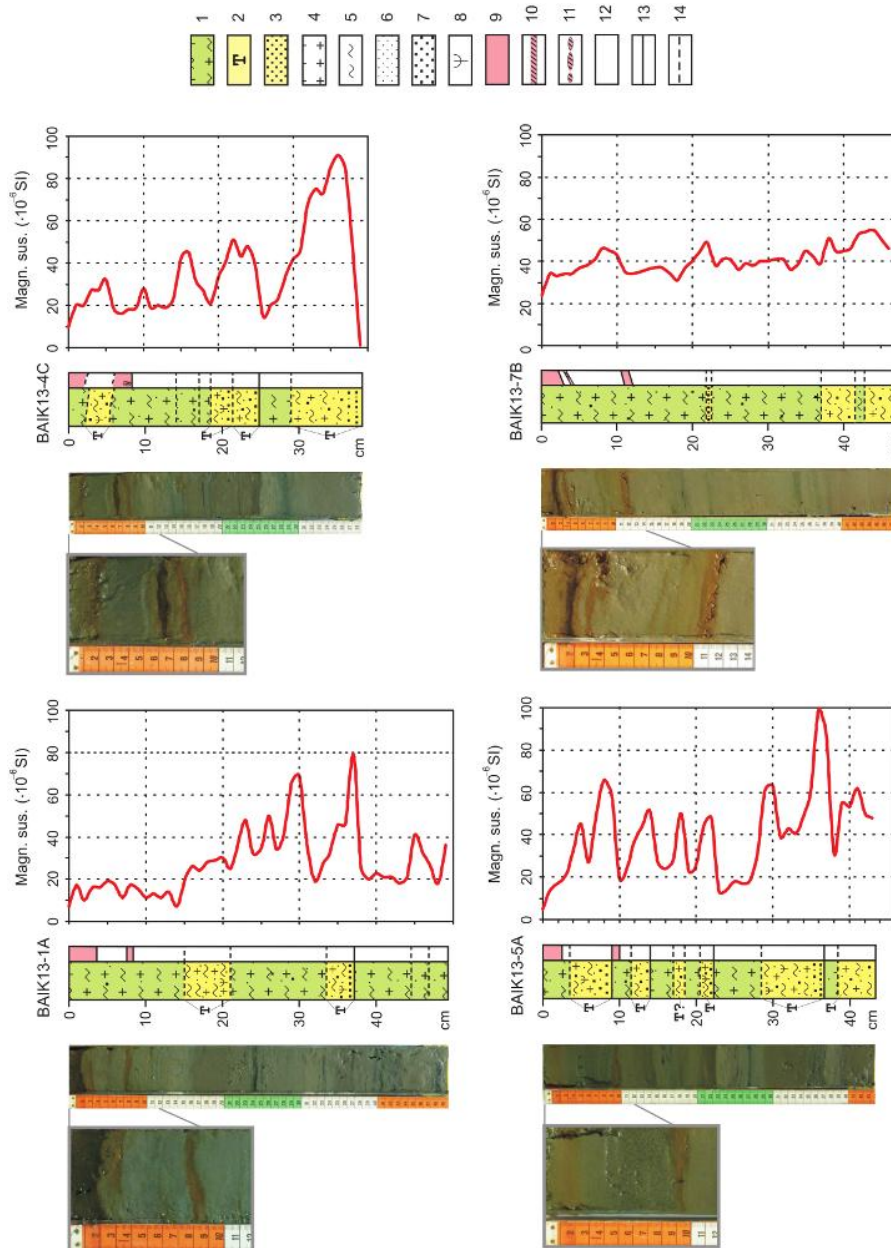
198 **3.1 Core lithology**

199 The deep water sediments of Lake Baikal are characterized by homogenous, fine-grained, and grey to olive-
 200 grey pelagic muds. They primarily consist of autochthonous biogenic material (mainly diatoms) with small
 201 amounts of allochthonous, terrigenous material (including pollen grains, clayey silts and a few sand grains).

202 The entire water column of Lake Baikal is saturated throughout with oxygen, due to the regular renewal of the
 203 deep waters (Shimaraev et al., 1994; Tsimitri et al., 2015), which results in the oxidation of even the deepest
 204 surface sediment. Cores BAIK13-1A, BAIK13-4C, BAIK13-5A and BAIK13-7B are oxidized down to a depth
 205 of 2.0-3.6 cm, showing olive-brown, dark-brown to brownish-black colours (Fig. 2). Core BAIK13-7B
 206 recovered closer to the southern shore of the south basin consists of slightly more coarse-grained sediments
 207 with an increased content of silt and sand (Fig. 2). The homogenous pelagic muds of the deep-water basins of
 208 the lake are frequently intercalated by coarse turbidite layers. These graded beds are characterized by
 209 allochthonous, mostly terrigenous material, higher magnetic susceptibility and a graded texture, which grades
 210 upwards from a sandy base to silty-pelitic deposits with few sand admixtures and occasionally overlain at the
 211 top by a thin pelitic mud layer (Vologina et al., 2007; Sturm et al., 2016).

212

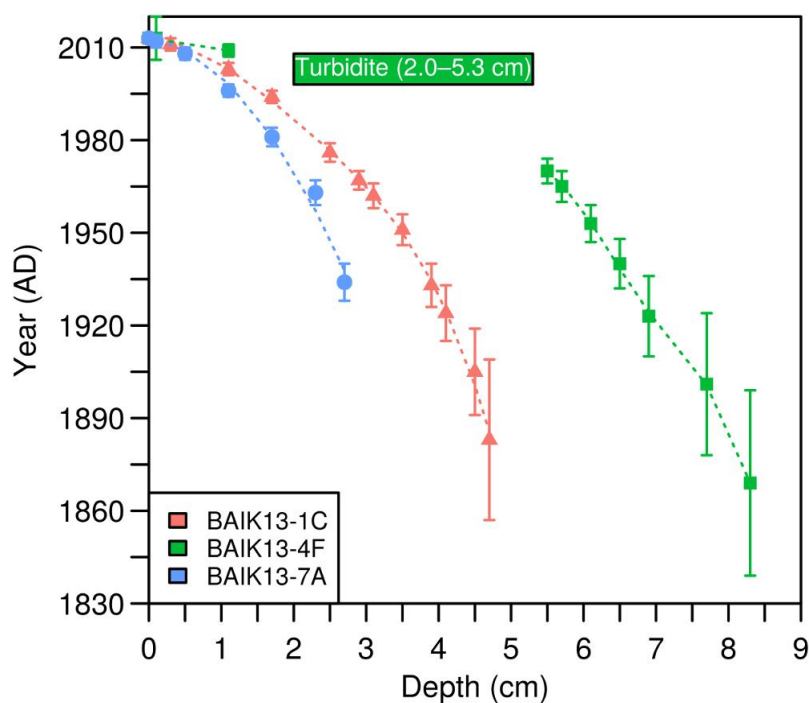
213 Several turbidites at different core depths and various thicknesses between 1.8 cm and 9.0 cm were observed in
 214 the cores, with two turbidites in BAIK13-1A, three in BAIK13-4C and six in BAIK13-5A (Fig. 2). The
 215 uppermost turbidites occur at 15.0–21.0 cm (BAIK13-1A), 2.0–5.3 cm (BAIK13-4C) and 3.5–9.0 cm
 216 (BAIK13-5A). There are layers of sand (21.8–22.5 cm) and sandy sediments (37.0–41.5 cm, 42.5–47.2 cm)
 217 without graded texture within sediment core BAIK13-7B. Lithological descriptions and MS-results were used
 218 to aid sampling of pelagic biogenic sediments (MS-values of up to 30×10^{-6} SI units) and avoid both turbidites
 219 and sandy layers (MS-values of up to 99×10^{-6} SI units).



220 Figure 2: Photos, lithology and magnetic susceptibility of sediment cores BAIK13-1A, BAIK13-4C, BAIK13-
 221 5A and BAIK13-7B from the south basin of Lake Baikal. Lithology (left column): 1 - pelagic mud, 2 -
 222 turbidite, 3 - sandy sediment, 4 - diatoms, 5 - clay, 6 - silt, 7 - sand, 8 - land plant remains. Right column: 9 -
 223 oxidized sediment, 10 - Fe/Mn crust, 11 - fragments of Fe/Mn crust, 12 – O₂ reduced sediment. Boundaries
 224 between layers: 13 - distinct boundaries between layers, 14 - indistinct boundaries between layers.

225 **3.2 ^{210}Pb age models**

226 Total ^{210}Pb activity reaches equilibrium with supported ^{210}Pb at a depth of c. 5 cm (BAIK13-1C), 9 cm
 227 (BAIK13-4F) and 4 cm (BAIK13-7A). At sites BAIK13-1C and BAIK13-4F well resolved peaks of ^{137}Cs at 3.1
 228 cm and 5.5-5.7 cm respectively likely relate to peak atmospheric testing of nuclear weapons 1963 AD. At all
 229 sites, non-monotonic variation in unsupported ^{210}Pb prevented the use of the constant initial concentration (CIC)
 230 dating model. Instead, ^{210}Pb dates were calculated using the constant rate of ^{210}Pb supply (CRS) model
 231 (Appleby and Oldfield, 1978). At BAIK13-1C and BAK13-4F depths of 3.1 cm and 5.7 cm are dated to
 232 1962/1963 AD respectively, both in agreement with the ^{137}Cs record. An absence of clear peaks in either ^{137}Cs or
 233 ^{241}Am at BAIK13-7A prevents validation of the ^{210}Pb dates. For all sites the final age-depth model shows a good
 234 fit to the ^{210}Pb dates (BAIK13-1C Adjusted $R^2 > 0.99$; BAIK13-4F Adjusted $R^2 = > 0.99$; BAK13-7A Adjusted
 235 $R^2 > 0.99$) (Fig. 3). Mean uncertainty in the individual ^{210}Pb dates across all three cores is 6.8 years (BAIK13-
 236 1C: $\bar{x} = 7$, range = 2-26; BAIK13-4F: $\bar{x} = 8$, range = 2-30; BAIK13-7A: $\bar{x} = 3$, range = 2-6) (Fig. 3).



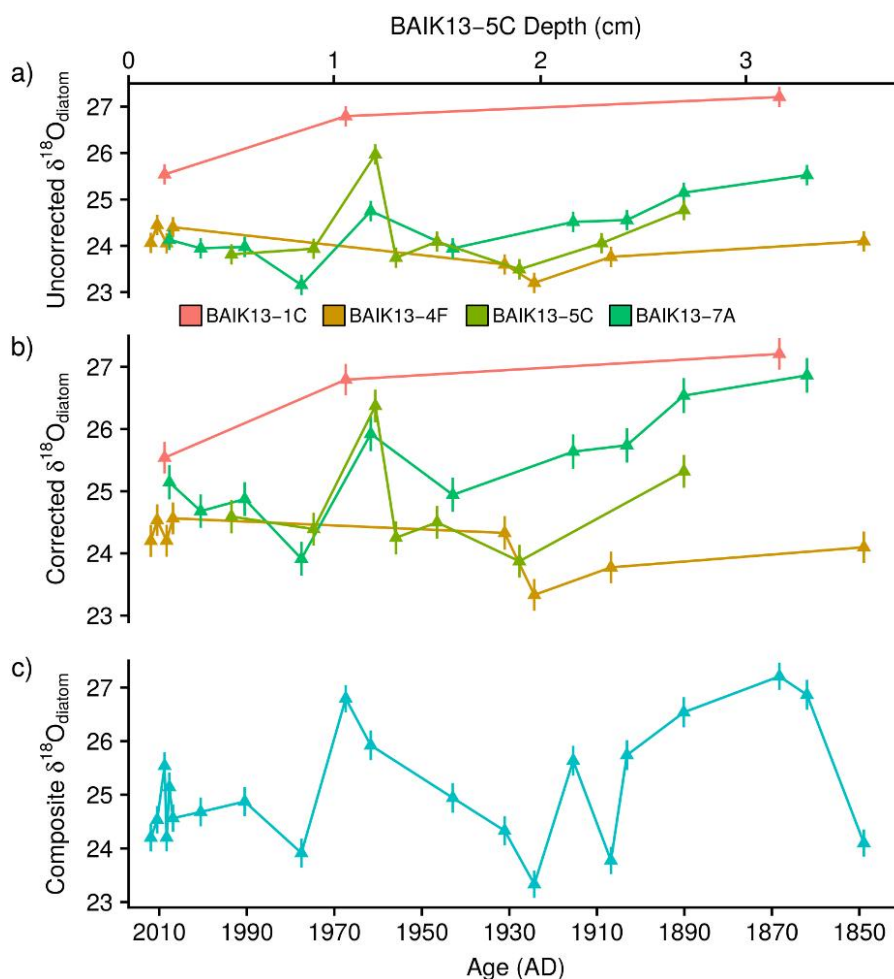
237 Figure 3: ^{210}Pb age-depth models for cores BAIK13-1C, BAIK13-4F and BAIK13-7A.

238

239 **3.3 $\delta^{18}\text{O}_{\text{diatom}}$**

240 Analysed samples from the four sediment cores cover the interval from c. 2010-1850 AD with raw $\delta^{18}\text{O}_{\text{diatom}}$
 241 varying from +23.2‰ to +28.1‰ and replicate analyses of sample material indicating an analytical
 242 reproducibility (1σ) of 0.2‰ (Fig. 4a). Results from BAIK13-5C, which does not have an age model, display
 243 similar values and variations to those in BAIK13-4F and BAIK13-7C, although values at BAIK13-1C are

244 notably higher at +25.5‰ to +27.2‰. Levels of contamination were minimal for cores BAIK13-1C (\bar{x} = 0%
 245 contamination), BAIK13-4F (\bar{x} = 1.7% contamination) and BAIK13-5C (\bar{x} = 3.9% contamination) with Al/Si
 246 ratios of <0.02. At BAIK13-7C Si/Al ratios increase to 0.018-0.027 (\bar{x} = 0.023) indicating the need to account
 247 for aluminosilicates. Following correction for contaminants on samples at all sites, $\delta^{18}\text{O}_{\text{diatom}}$ ranges from
 248 +23.3‰ to +27.2‰ (\bar{x} = +24.5‰, 1σ = 1.0‰) (Fig. 4b) with the propagation of error associated with the
 249 correction increasing the analytical uncertainty for individual samples to 0.25-0.28‰. The two samples without
 250 XRF data are not considered further in this manuscript and all further mention of $\delta^{18}\text{O}_{\text{diatom}}$ refers to the
 251 corrected $\delta^{18}\text{O}_{\text{diatom}}$ dataset (Supplementary Table 1).



252 Figure 4: $\delta^{18}\text{O}_{\text{diatom}}$ from the south basin of Lake Baikal. Raw (uncorrected) (A) and corrected (B) $\delta^{18}\text{O}_{\text{diatom}}$
 253 together with the composite south basin $\delta^{18}\text{O}_{\text{diatom}}$ record (C). All samples plotted against age except for
 254 BAIK13-5C, which are plotted against depth and not used in the final composite $\delta^{18}\text{O}_{\text{diatom}}$ record. Error bars for
 255 uncorrected $\delta^{18}\text{O}_{\text{diatom}}$ data are the 1σ analytical reproducibility (0.2‰) with error bars for the corrected $\delta^{18}\text{O}_{\text{diatom}}$
 256 data reflecting the propagation of error associated with the correction for contaminants (range = 0.25-0.28‰).

257

258 On the basis of homogeneity in $\delta^{18}\text{O}_{\text{water}}$ across the modern lake and through the water column (Seal and

259 Shanks, 1998; Morley et al., 2005), $\delta^{18}\text{O}_{\text{diatom}}$ data from sites BAIK13-1C, BAIK13-4F and BAIK13-7C are
260 combined to create a composite record of south basin $\delta^{18}\text{O}_{\text{diatom}}$ ranging from +23.3‰ to +27.2‰ (\bar{x} = +25.1‰,
261 1σ = 1.1) (Fig. 4c). After c. 1850 (+24.1‰), $\delta^{18}\text{O}_{\text{diatom}}$ increases in the second half of the 19th century to higher
262 values of +25.1‰ to +27.2‰. Through the 20th century $\delta^{18}\text{O}_{\text{diatom}}$ is variable (\bar{x} = +24.2‰, 1σ = 1.1‰),
263 particularly from 1960-1970 when $\delta^{18}\text{O}_{\text{diatom}}$ reaches a minimum of +23.2‰ by the end of the 1970's and a peak
264 of +26.8‰ in the late 1960's. Values of $\delta^{18}\text{O}_{\text{diatom}}$ in the decade before the cores were collected in 2013 vary
265 from +24.1‰ to +25.5‰ (\bar{x} = +24.5‰, 1σ = 0.6‰).

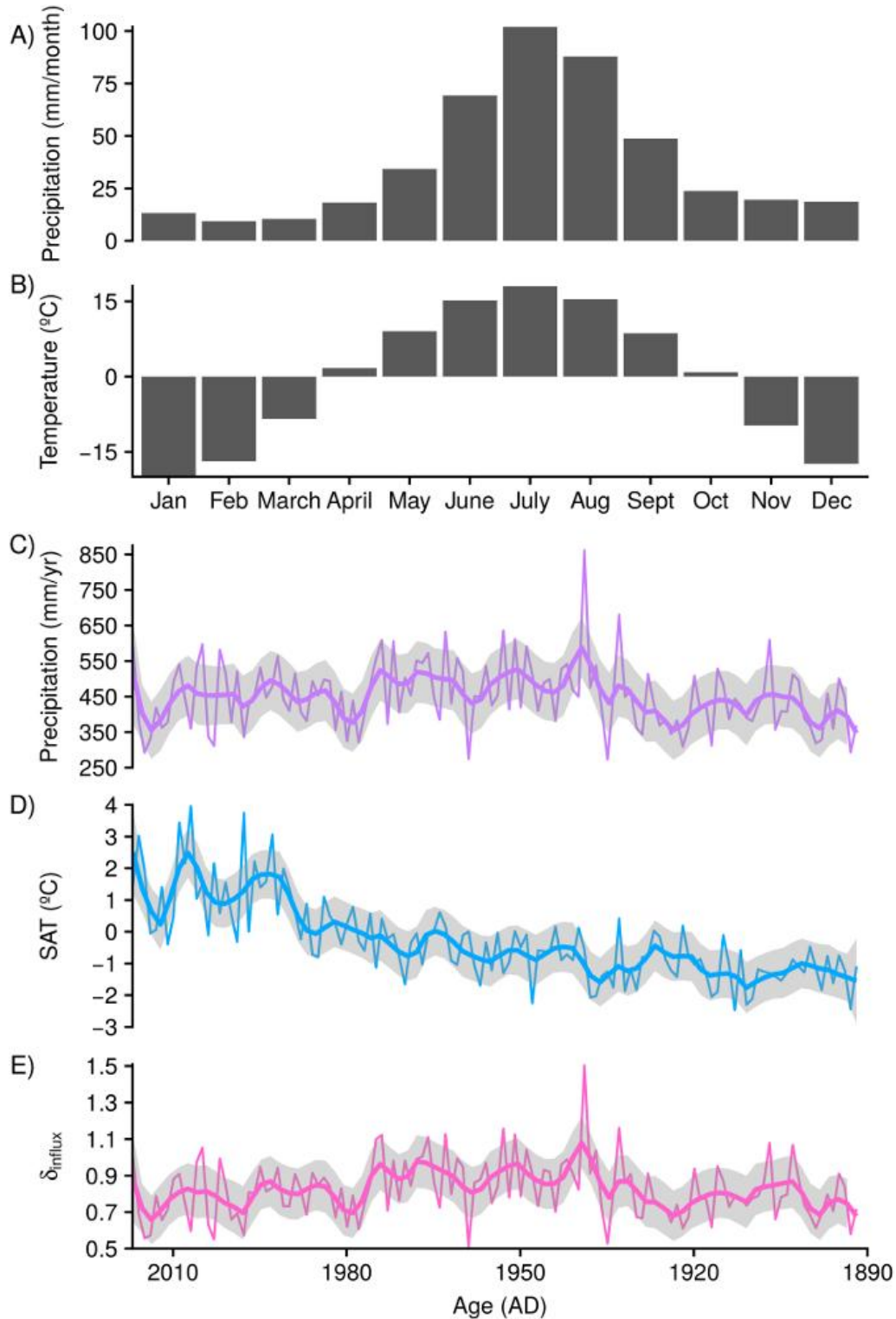
266

267 **3.4 δ_{influx}**

268 Mean annual precipitation in Irkutsk is 450 mm/yr with c. 75% of precipitation falling in the extended summer
269 period from May to September, and only <10% falling in winter (DJF) (Fig. 5a). Surface air temperatures show
270 similar seasonal variations from -20°C in January to +18°C in July (Fig. 5b). No systematic change in
271 precipitation is apparent for recent decades, although precipitation from 2016-1926 (\bar{x} = 466 mm/yr) is notably
272 higher than 1925-1891 (\bar{x} = 410 mm/yr, $p < 0.001$) after the step change in 1926 (Fig. 5c). In line with global
273 records, SAT at Irkutsk show a prolonged warming trend over the monitoring record with marked increases
274 from c. 1950 and c. 1990 onwards that are predominantly associated with increases in winter SAT (Fig. 5d).
275 Annual and seasonal trends in precipitation and SAT from Irkutsk are similar to data from other sites around
276 Lake Baikal, with similar trends observed in records of water inflow to the lake (Shimaraev et al., 2002;
277 Frolova et al., 2017). As such, the meteorological data from Irkutsk can be regarded as being representative of
278 the wider region.

279

280 Values of δ_{influx} shows mean inter-annual variations of c. 0.17 from 2016-1891 (Fig. 5e). On decadal timescales,
281 from 1923-1891 δ_{influx} varies by c. 0.58 (\bar{x} = 0.79‰, 1σ = 0.13) before a long-term increase to the maxima in
282 1938 of 1.50, caused by exceptionally high June 1938 rainfall of 318 mm. Thereafter, values reveal a long-term
283 decline from mean 1970-1950 values of c. 0.9 to mean values of 0.77 since the year 2000.



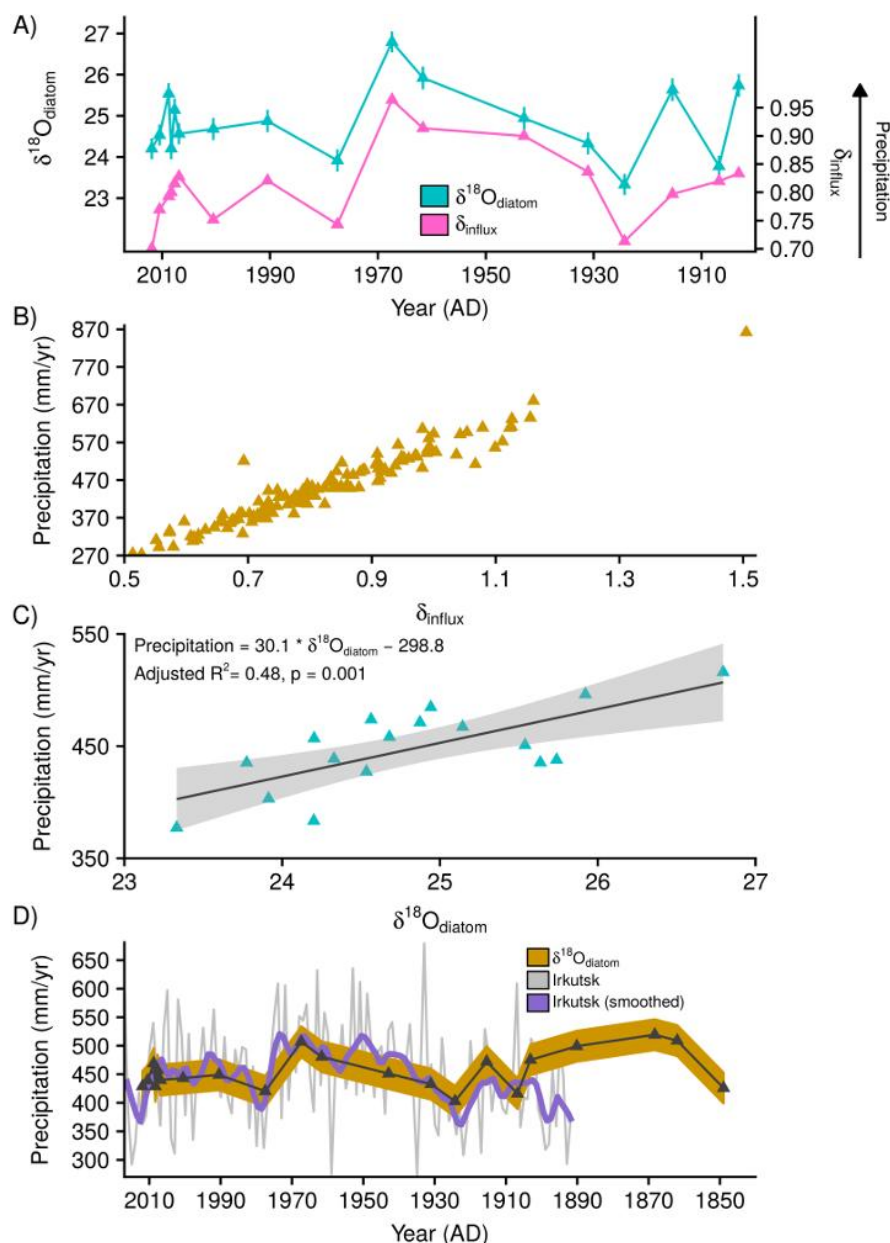
284 Figure 5: Meteorological data from Irkutsk (World Meteorological Organisation station 30710) showing the (A)
 285 monthly distribution of precipitation and (B) surface air temperature (SAT) alongside (C) temporal changes in
 286 precipitation and (D) surface air temperature from 2016-1891. Values of δ_{influx} (E) are calculated following
 287 Equations 1 and 2 with all values normalised relative to a value of 1 for 2016 AD. Thicker lines for panels C-E
 288 show locally weighted smoothing (loess) with shaded regions representing the 95% confidence interval on the
 289 fitted values.

290 **3.5 Comparison of $\delta^{18}\text{O}_{\text{diatom}}$ and δ_{influx}**

291 To account for uncertainty in the age-model and with analysed samples containing diatoms that accumulated
292 over multiple years, a locally-weighted polynomial regression (lowess) was applied to δ_{influx} with a span of 10
293 years in order to enable robust comparisons with $\delta^{18}\text{O}_{\text{diatom}}$. From c. 2010-1900 change in $\delta^{18}\text{O}_{\text{diatom}}$ are
294 significantly correlated to δ_{influx} ($r = 0.72$ $p = 0.001$) with a linear regression revealing a significant relationship
295 between the two variables (Adjusted $R^2 = 0.48$, $p = 0.001$) (Fig. 6a). Whilst the residence time of water in the
296 south basin is closer to 80-90 years (Shimaraev et al., 1994), the age of surface waters down to the mesothermal
297 maximum (200–300 m water depth) are likely to be less, given reduced rates of mixing with deep/bottom
298 waters (Weiss et al., 1991). The duration of vertical exchanges across the lake is limited to a short timeframe
299 each year, with rates varying spatially across individual basins and between coastal and non-coastal sites (Weiss
300 et al., 1991; Shimaraev et al., 1994; Ravens et al., 2000; Shimaraev et al., 2012; Troitskaya et al., 2015). With
301 the mechanisms and extent of vertical mixing across Lake Baikal therefore remaining relatively unconstrained,
302 it becomes impossible to accurately model the age of the ambient water in which the analysed diatoms
303 photosynthesised. The span of 10 year employed in the regression of δ_{influx} is considered to be an appropriate
304 estimate for this, given that surface $\delta^{18}\text{O}_{\text{water}}$ is likely to be significantly weighted towards more recent inputs to
305 the lake.

306

307 Variance partitioning of δ_{influx} against surface air temperature and precipitation data from Irkutsk reveals 94% of
308 the variability in δ_{influx} is related to changes in precipitation. This is confirmed by the strong relationship
309 between δ_{influx} and annual precipitation at Irkutsk from 2016-1891 AD and hence between decadal smoothed
310 annual precipitation (span = 10 years) and $\delta^{18}\text{O}_{\text{diatom}}$ (Adjusted $R^2 = 0.48$, $p = 0.001$, $SE = 26.9$ mm/yr) (Fig. 6
311 b,c). In contrast, there is no relationship between $\delta^{18}\text{O}_{\text{diatom}}$ and air temperatures at Irkutsk. From this
312 relationship between $\delta^{18}\text{O}_{\text{diatom}}$ and precipitation, quantitative reconstructions of decadal averaged annual
313 precipitation can be made from $\delta^{18}\text{O}_{\text{diatom}}$ with results, when applied to the south basin composite record,
314 ranging from c. 400-520 mm/yr with variations between samples of up to 80 mm (Fig. 6d). These reconstructed
315 estimates of precipitation are offset from actual measured levels of precipitation at Irkutsk by 5-45 mm/yr ($\bar{x} =$
316 22.6 mm/yr) (Fig. 6d).



317 Figure 6: A) Composite $\delta^{18}\text{O}_{\text{diatom}}$ and δ_{influx} from c. 2010-1900 AD showing the strong correlation ($r = 0.72$ $p =$
 318 0.001) and linear relationship (Adjusted $R^2 = 0.48$, $p = 0.001$) between the two variables. Displayed values of
 319 δ_{influx} are obtained from a locally weighted smoothing (span = 10 years) of the raw δ_{influx} data to account for
 320 uncertainty in the ^{210}Pb age model and accumulation of diatoms in the sediment record over multiple years. B)
 321 Relationship between raw δ_{influx} and Irkutsk annual precipitation from 2016-1891. C) Linear relationship
 322 between $\delta^{18}\text{O}_{\text{diatom}}$ and locally weighted Irkutsk precipitation (span = 10 years). D) Decadal annual precipitation
 323 reconstructed from $\delta^{18}\text{O}_{\text{diatom}}$ (brown region/black line) together with Irkutsk annual precipitation (grey) and
 324 locally weighted (span = 10 years) Irkutsk precipitation (purple). Shaded region for reconstructed precipitation
 325 is the standard error (26.9 mm/yr) of the regression model between $\delta^{18}\text{O}_{\text{diatom}}$ and Irkutsk precipitation (Fig. 6c).
 326 For clarity the y-axis has been scaled to not show the extreme Irkutsk precipitation of 861.9 mm^{-1} in 1938 AD.

327 **4 Discussion**328 **4.1 $\delta^{18}\text{O}_{\text{diatom}}$ as an indicator of Central Asian precipitation**

329 Both $\delta^{18}\text{O}_p$ and $\delta^{18}\text{O}_{\text{river}}$ in the Lake Baikal catchment fall on or close to the global meteoric water line (Seal and
330 Shanks, 1998) with evaporation believed to not significantly impact $\delta^{18}\text{O}_{\text{water}}$ (Morley et al., 2005). With
331 changes in the amount of precipitation dominating variations in δ_{influx} (Fig. 6b), δ_{influx} can be interpreted as
332 primarily reflecting decadal changes in annual precipitation and in particular summer precipitation which
333 accounts for 70-90% of annual precipitation to the region (Fig. 5b; Afanasjev, 1976; Shimaraev et al., 1994). As
334 $\delta^{18}\text{O}_{\text{diatom}}$ reflects the isotope composition of ambient water in Lake Baikal, sedimentary records of $\delta^{18}\text{O}_{\text{diatom}}$
335 should also reflect changes in regional Central Asian precipitation across the wider region around Lake Baikal.
336 This is supported by the strong correlation and relationship between δ_{influx} and $\delta^{18}\text{O}_{\text{diatom}}$, with increases
337 (decrease) in $\delta^{18}\text{O}_{\text{diatom}}$ associated with higher (lower) δ_{influx} and an increase (decrease) in precipitation (Fig. 6a),
338 as well as by the linear relationship between $\delta^{18}\text{O}_{\text{diatom}}$ and decadal smoothed annual precipitation (Fig. 6c).

339

340 Reanalysis data demonstrates that moisture transportation to the region throughout the year is primarily
341 dominated by westerlies which, along with the Siberian High, control intra-annual variations in precipitation
342 (Lydolph, 1977; Kurita et al., 2004), although we cannot rule out that other moisture sources may have become
343 more dominant in the past beyond the observational record. In spring, the intensification of zonal circulation
344 leads to the westerly progression of cyclones to the region, a process that intensifies in summer as low-pressure
345 systems continue to develop along the Asiatic polar front (Lydolph, 1977; Chen et al., 1991; Shahgedanova
346 2002). With summer precipitation and inter-annual variations within it closely linked to eastward-propagating
347 Rossby waves along the Asian Polar Front Jet (Iwao and Takahashi 2006, 2008), variations in summer Siberian
348 precipitation have been linked to the Atlantic Multidecadal Oscillation (AMO) (Sun et al., 2015). Related to sea
349 surface temperatures (SST) in the North Atlantic Ocean, the warm SST associated with a positive phase of the
350 AMO are proposed to enhance precipitation across Siberia through a northerly shift in Rossby waves. Records
351 of $\delta^{18}\text{O}_{\text{diatom}}$ from Lake Baikal can therefore now be employed to investigate long-term, decadal to centennial,
352 controls on summer precipitation including the link between precipitation and the AMO. Debate exists over the
353 extent to which the AMO will change in the future beyond natural fluctuations. Results from the IPCC AR5
354 report suggest that the AMO is unlikely to change its behaviour in a warmer climate state (Christensen et al.,
355 2013). However, comparisons have shown the complexity in ensuring models adequately capture the
356 characteristic of the AMO (Kavvada et al., 2013) whilst evidence exists for an amplification of the AMO at the

357 onset of industrial-era warming (Moore et al., 2017) and so the potential for further modifications with
358 increased SST.

359

360 On the basis of our composite $\delta^{18}\text{O}_{\text{diatom}}$ record from the south basin of Lake Baikal and the link to δ_{influx} and
361 $\delta^{18}\text{O}_p$ from 2011-1901 (Fig. 6a-c) we propose that $\delta^{18}\text{O}_{\text{diatom}}$ can be used to constrain annual precipitation and,
362 given the seasonal distribution of precipitation, the summer position of the Asiatic polar front and associated jet
363 system (Fig. 5b). This interpretation of $\delta^{18}\text{O}_{\text{diatom}}$ does not contradict previous records from Lake Baikal which
364 related changes in $\delta^{18}\text{O}_{\text{diatom}}$ to the balance of north and south basin river inputs in Lake Baikal and so the wider
365 hydroclimate of the region (Mackay et al., 2008, 2011, 2013). Instead, the relationship observed here now
366 permits an enhanced understanding of the palaeoclimatology of the region by disentangling the dominant
367 environmental controls on $\delta^{18}\text{O}_{\text{diatom}}$, precipitation and lake water temperature, allowing the quantification of
368 past changes in Central Asia precipitation.

369

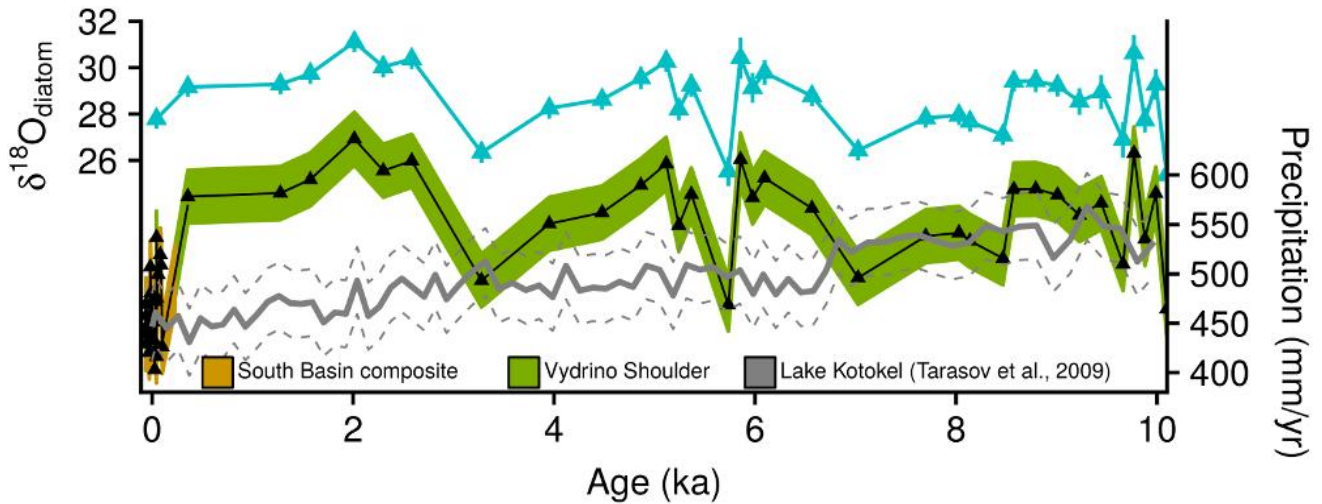
370 **4.2 Holocene reconstruction of Central Asian precipitation**

371 Precipitation data from Irkutsk is not available prior to 1891. Using the relationship between $\delta^{18}\text{O}_{\text{diatom}}$ and
372 precipitation from c. 2010-1900 (Fig. 6c) we quantify decadal changes in annual precipitation for Central Asia
373 from our composite south basin $\delta^{18}\text{O}_{\text{diatom}}$ record, which extends back to c. 1850 AD (Fig. 6d). Results show that
374 the degree of variability in 21st and 20th century precipitation also prevailed through the late 19th century (426-
375 519 mm/yr) with significantly lower levels of precipitation in c. 1850 relative to 1860-1890. Within the
376 constraints of this low-resolution record and the regression standard error of 26.9 mm/yr, the results suggest
377 that decadal annual precipitation in Central Asia has not notably changed in response to increased
378 global/regional air temperature over the last c. 160 years (Fig. 6d). Observed reductions in Central Asian
379 precipitation and river flow over recent decades (Liu et al., 2013; Li et al., 2015; Frolova et al., 2017) may
380 therefore represent natural variability rather than an anthropogenic driven change.

381

382 Tree ring records from Mongolia currently provide regional hydroclimate data for the last 500 years (Pederson
383 et al., 2001; Davi et al., 2006, 2009, 2010; Seim et al., 2017). However, longer precipitation records are needed,
384 particularly over abrupt climate transitions and from geological analogues for the future to fully assess trends in
385 Central Asian precipitation and possible links to the North Atlantic region. To place the results of the composite
386 south basin core over the last c. 200 years within the context of natural variability, long-term changes in Central

387 Asian precipitation are reconstructed from a previously published corrected $\delta^{18}\text{O}_{\text{diatom}}$ record from Vydrino
 388 Shoulder (51.588N, 104.858E, Fig. 1) located off the southern shoreline of Lake Baikal (Mackay et al., 2011)
 389 using our $\delta^{18}\text{O}_{\text{diatom}}$ /precipitation calibration. The range of $\delta^{18}\text{O}_{\text{diatom}}$ in the core from Vydrino Shoulder (+25.3‰
 390 to +31.1‰) (Fig. 7) is similar to that observed at nearby Lake Kotokel (+23.7‰ to +36‰), despite the
 391 significantly different controls and isotope setting of this smaller lake (Kostrova et al., 2013) (Fig. 1).



392 Figure 7: Holocene $\delta^{18}\text{O}_{\text{diatom}}$ from Vydrino Shoulder (51.588N, 104.858E, Fig. 1) located off the southern
 393 shoreline of Lake Baikal (Mackay et al., 2011) together with reconstructed precipitation at Vydrino Shoulder
 394 (green) and in the south basin composite record (brown) displayed in Figure 6d. One sample from the Vydrino
 395 Shoulder core (0.04 ka / 1907 AD) overlaps with the composite record in Figure 6. Shaded region shows range
 396 of reconstructed precipitation based on the standard error (26.9 mm/yr) of the regression model between
 397 $\delta^{18}\text{O}_{\text{diatom}}$ and Irkutsk precipitation (Fig. 6c). Also shown is the pollen inferred precipitation record from Lake
 398 Kotokel (solid grey line) (Tarasov et al., 2009) and the associated root mean square error of prediction (RMSE)
 399 of 34 mm/yr (Solovieva et al., 2005).

400

401 From 0-10 ka annual precipitation reconstructed from Vydrino Shoulder ranges from c. 470-640 mm/yr (\bar{x} =
 402 565 mm/yr, 1σ = 40 mm/yr) (Fig. 7). No decline in precipitation occurs from c. 0.2-4.0 ka, but significant
 403 variability is apparent through the mid-Holocene warm interval from 5-9 ka (\bar{x} = 558 mm/yr, 1σ = 41 mm/yr).
 404 The record is notable in displaying values of precipitation that are markedly higher than those recorded at
 405 Irkutsk during the 20th and 21st Century, with values only comparable to mean modern day conditions (450 mm/
 406 yr) at 3.3 ka, 5.7 ka and 10.1-10.2 ka (Fig. 7). However, for 50% of the samples reconstructed $\delta^{18}\text{O}_{\text{diatom}}$
 407 precipitation and their standard error fit with the range of Lake Kotokel pollen derived precipitation and their
 408 associated error (Tarasov et al., 2009) (Fig. 1, 7). This similarity between pollen and $\delta^{18}\text{O}_{\text{diatom}}$ precipitation is

409 most apparent in the early Holocene. In contrast, $\delta^{18}\text{O}_{\text{diatom}}$ precipitation is significantly higher than pollen
410 precipitation for most of the mid/late Holocene interval.

411

412 *4.2.1 Assessing the fidelity of the Holocene $\delta^{18}\text{O}_{\text{diatom}}$ record*

413 It is necessary to consider possible issues that may have impacted the $\delta^{18}\text{O}_{\text{diatom}}$ record at Vydrino Shoulder
414 given: 1) the mismatch between $\delta^{18}\text{O}_{\text{diatom}}$ and pollen derived precipitation during the mid/late Holocene; and 2)
415 reconstructed $\delta^{18}\text{O}_{\text{diatom}}$ precipitation values from Vydrino Shoulder which are notably higher than those from
416 the south basin composite record (Fig. 7). Diatom dissolution in Lake Baikal can be significant, with only 1%
417 of diatoms preserved in the sediment record (Ryves et al., 2003; Battarbee et al., 2005). Of those preserved,
418 dissolution indices indicate that 40-60% of all frustules over the last 1000 years show some form of dissolution
419 (Mackay et al., 1998), increasing to 60-90% for MIS 5e (Rioual and Mackay, 2005). Despite this and the
420 potential for samples from Vydrino Shoulder to have experienced higher rates of dissolution, work has
421 conclusively shown that dissolution does not impact the silicon isotope signature in diatoms from Lake Baikal
422 (Panizzo et al., 2016). In addition, laboratory experiments on a sample from Lake Baikal have shown that
423 increased dissolution does not vary $\delta^{18}\text{O}_{\text{diatom}}$ beyond analytical error (Smith et al., 2016). Based on this, there is
424 no evidence that the $\delta^{18}\text{O}_{\text{diatom}}$ signature in either the south basin composite record or the Vydrino Shoulder
425 record is impacted by dissolution or other post-depositional processes.

426

427 The $\delta^{18}\text{O}_{\text{diatom}}$ reconstructed precipitation is also unlikely to be affected by Holocene changes in air temperature
428 due to: 1) its negligible impact on δ_{influx} and $\delta^{18}\text{O}_{\text{diatom}}$ (Section 3.5); and 2) pollen derived reconstructions from
429 both Lake Kotokel and the north basin of Lake Baikal that display “warmest month” temperature variations of
430 only 2°C through the Holocene (Tarasov et al., 2007, 2009). The $\delta^{18}\text{O}_{\text{diatom}}$ /precipitation calibration assumes that
431 both the moisture source region and the relative contribution of rivers flowing into Lake Baikal together with
432 their seasonality has not significantly altered through the Holocene. Relative increase in winter
433 precipitation/snow melt therefore has the potential to distort (lower) reconstructed precipitation due to the lower
434 $\delta^{18}\text{O}_{\text{water}}$ that arises from colder atmospheric temperatures (Seal and Shanks, 1998). A similar effect may occur
435 with significant increases in the relative inflow of more northerly rivers, such as the Upper Angara and
436 Barguzin Rivers, given modern $\delta^{18}\text{O}_{\text{river}}$ compositions that are 4-6‰ lower than those for the Selenga River
437 (Seal and Shanks, 1998). However, with summer precipitation accounting for 70-90% of annual precipitation
438 (Fig. 5b; Afanasjev, 1976; Shimaraev et al., 1994) and with 62% of modern riverine inflow originating from the

439 Selenga River, it is difficult to envisage that Holocene hydrological conditions deviated sufficiently to alter
440 $\delta^{18}\text{O}_{\text{diatom}}$ and the robustness of the $\delta^{18}\text{O}_{\text{diatom}}$ /precipitation calibration.

441 Based on the above and current knowledge on both $\delta^{18}\text{O}_{\text{water}}$ and $\delta^{18}\text{O}_{\text{diatom}}$ in Lake Baikal, it is not possible to
442 attribute the mid/late Holocene offset between $\delta^{18}\text{O}_{\text{diatom}}$ and pollen precipitation reconstructions to
443 methodological or proxy calibration issues. Instead, both the pollen and $\delta^{18}\text{O}_{\text{diatom}}$ reconstructions need to be
444 considered as providing complementary information on precipitation trends across the catchment. When
445 comparing the $\delta^{18}\text{O}_{\text{diatom}}$ precipitation reconstruction from Vydrino Shoulder to other records from the region, it
446 is notable that results are broadly comparable to patterns of effective summer precipitation obtained from a
447 low-resolution regional general circulation model (Bush, 2005). Pollen precipitation reconstructions from both
448 Lake Baikal and Lake Kotokel display similar trends to one another through the Holocene (Tarasov et al., 2007,
449 2009) with the divergence away from $\delta^{18}\text{O}_{\text{diatom}}$ precipitation emerging after c. 7 ka, when pollen precipitation
450 decreases by c. 10% with no corresponding change in $\delta^{18}\text{O}_{\text{diatom}}$ precipitation (Fig. 7). This decline in pollen
451 precipitation around Lake Baikal also contrasts with records from the northern Mongolian Plateau (in the
452 southern extent of the lake's catchment) which, similar to the $\delta^{18}\text{O}_{\text{diatom}}$ precipitation record from Vydrino
453 Shoulder, show high rates of annual precipitation in both the early and late Holocene (Wang and Feng, 2013).
454 Although records on the northern Mongolian plateau show a degree of spatial variability, no long-term decline
455 in precipitation is apparent from c. 7 ka (Wang and Feng, 2013). Although it is beyond the remit of this study to
456 evaluate the robustness of the pollen reconstructions, it is suggested that existing pollen records from Lake
457 Baikal and Lake Kotokel (Tarasov et al., 2007, 2009) may reflect localised, site-specific, changes in
458 precipitation. In contrast, given the size of Lake Baikal's catchment (540,000 km²) and with 83% of riverine
459 inflow originating from the Selenga River and its tributaries, which extend into Mongolia, or the Upper Angara
460 and Barguzin Rivers, which drain the region immediately to the east and north of Lake Baikal (Fig. 1), we
461 propose that our $\delta^{18}\text{O}_{\text{diatom}}$ precipitation record from Lake Baikal reflects an amalgamated average of conditions
462 across the wider Central Asian region incorporating the lake's catchment. If correct, this interpretation suggests
463 that whilst pollen records indicate drier conditions immediately around Lake Baikal in the mid/late Holocene
464 (Tarasov et al., 2007, 2009), the higher $\delta^{18}\text{O}_{\text{diatom}}$ records imply that long-term trends in precipitation elsewhere
465 in the catchment and in particular to the south of the lake remained relatively constant between the early/late
466 Holocene period, trends that are supported by individual records from northern Mongolian (Wang and Feng,
467 2013).

469 With a relationship established between $\delta^{18}\text{O}_{\text{diatom}}$ and regional Central Asian precipitation around Lake Baikal,
470 records of precipitation from the lake have the potential to aid the development of future forecasts for the
471 region. Models in the Coupled Model Intercomparison Project (CMIP5) are currently not able to confidently
472 predict future changes in Central Asian precipitation (Christensen et al., 2013), but together with regional
473 models they indicate the potential for decreases in precipitation for northern Mongolia and the Lake Baikal
474 catchment, leading to associated reductions in soil moisture and increased vulnerability to drought and fire
475 (Sato et al., 2007; Törnqvist et al., 2014). Data-model comparisons under the Paleoclimate Modelling
476 Intercomparison Project (PMIP) highlight the complexities in generating accurate simulation of precipitation
477 for the mid-Holocene (Bartlein et al., 2010; Braconnot et al., 2012). Whereas PMIP3 simulations suggest that
478 regional conditions were drier in the mid-Holocene compared to pre-industrial conditions (Bartlein et al.,
479 2017), our low-resolution results suggest that regional precipitation at 6 ka was c. 25% higher than modern
480 (450 mm/yr) and c. 30% higher than reconstructed precipitation of 430 mm/yr in pre-industrial conditions at c.
481 1850 AD (Fig. 7). Further investigations on the controls of $\delta^{18}\text{O}_{\text{diatom}}$ in Lake Baikal, in an attempt to better
482 constraint the divergence with pollen reconstructed precipitation through the mid/late Holocene, together with
483 higher resolution measurements through the Holocene and integration of these results within ongoing
484 modelling efforts therefore holds the potential to aid future model validations for Central Asia. In particular,
485 higher resolution records will provide greater insight into the abrupt changes in precipitation that are
486 superimposed on the Holocene record from Vydrino Shoulder, events that may be concordant with ice-rafted
487 debris events in the North Atlantic Ocean (Mackay et al., 2011).

488

489 **5 Conclusions**

490 There is uncertainty over the potential for future changes in Central Asian precipitation under a warmer climate
491 state, changes which have severe implications for the grassland-taiga ecotone and carbon cycling in the region.
492 By comparing records of $\delta^{18}\text{O}_{\text{diatom}}$ to local meteorological data for the last 100 years we demonstrate an
493 empirical relationship in Lake Baikal between $\delta^{18}\text{O}_{\text{diatom}}$ and Central Asian precipitation, providing an
494 opportunity to study the long-term variability of regional precipitation. Accordingly, $\delta^{18}\text{O}_{\text{diatom}}$ records from
495 Lake Baikal have the potential to aid future climate predictions by investigating geological intervals that might
496 represent an analogue of a future climate state and through data-model comparisons. Results here from
497 Holocene measurements of $\delta^{18}\text{O}_{\text{diatom}}$ show that precipitation has varied significantly over the last 10 ka,
498 indicating the region's potential sensitivity to a perturbation in the climate system, with levels of precipitation

499 over the past c. 160 years either at or close to their lowest levels of the last 10 ka.

500

501 References

- 502 Afanasyev, A.N., 1976. The Water Resources and Water Balance of Lake Baikal Basin. Nauka Publishers, Novosibirsk. (in
503 Russian).
- 504 Appleby, P.G., Oldfield, F., 1978. The calculation of ^{210}Pb dates assuming a constant rate of supply of unsupported ^{210}Pb to
505 the sediment. *Catena* 5, 1-8.
- 506 Appleby, P.G., Nolan, P.J., Gifford, D.W., Godfrey, M.J., Oldfield, F., Anderson, N.J., Battarbee, R.W., 1986. ^{210}Pb dating by
507 low background gamma counting. *Hydrobiologia* 141, 21-27.
- 508 Appleby, P.G., Richardson, N., Nolan, P.J., 1992. Self-absorption corrections for well-type germanium detectors. *Nucl.*
509 *Instrum, Meth, B.* 71, 228-233.
- 510 Bartington Instruments 1995. Operation Manual MS2. Bartington Instruments, Oxford,
511 <http://www.bartington.com/Literaturepdf/Operation%20Manuals/om0408%20MS2.pdf>.
- 512 Bartlein, P.J., Harrison, S.P., Brewer, S., Connor, S., Davis, B.A.S., Gajewski, K., Guiot, J., Harrison-Prentice, T.I.,
513 Henderson, A., Peyron, O., Prentice, I.C., Scholze, M., Seppä, H., Shuman, B., Sugita S., Thompson, R.S., Viau, A.E.,
514 Williams, J., Wu, H., 2010. Pollen-based continental climate reconstructions at 6 and 21 ka: a global synthesis. *Clim.*
515 *Dyn.* 3-4, 775-802.
- 516 Bartlein, P.J., Harrison, S.P., Izumi, K., 2017., Underlying causes of Eurasian midcontinental aridity in simulations of mid-
517 Holocene climate, *Geophys. Res. Lett.* 44, 9020-9028.
- 518 Battarbee, R.W., Mackay, A.W., Jewson, D., Ryves, D.B., Sturm, M., 2005., Differential dissolution of Lake Baikal
519 diatoms: correction factors and implications for palaeoclimatic reconstruction. *Global Planet Change.* 46,75-86.
- 520 Braconnot, P., Harrison, S.P., Kageyama, M., Bartlein, P.J., Masson-Delmotte, V., Abe-Ouchi, A., Otto-Bliesner, B., Zhao,
521 Y., 2012., Evaluation of climate models using palaeoclimatic data. *Nat. Clim. Change* 2, 417-424.
- 522 Brewer, T., Leng, M., Mackay, A.W., Lamb, A., Tyler, J., Marsh, N., 2008. Unravelling contamination signals in biogenic
523 silica oxygen isotope composition: the role of major and trace element geochemistry. *J Quaternary Sci.* 23, 365-374.
- 524 Bush, A.B.G., 2005. $\text{CO}_2/\text{H}_2\text{O}$ and orbitally driven climate variability over central Asia through the Holocene. *Quatern. Int.*
525 136, 15-23.
- 526 Chaplignin, B., Leng, M.J., Webb, E., Alexandre, A., Dodd, J.P., Ijiri, A., Lücke, A., Shemesh, A., Abelmann, A.,
527 Herzschuh, U., Longstaffe, F.J., Meyer, H., Moschen, R., Okazaki, Y., Rees, N., Sharp, Z.D., Sloane, H.J., Sonzogni, C.,
528 Swann, G.E.A., Sylvestre, F., Tyler, J.T., Yam, R., 2011. Inter-laboratory comparison of oxygen isotopes from biogenic
529 silica. *Geochim. Cosmochim. Ac.* 75, 7242-7256.
- 530 Chen, S-J., Kuo, Y-H., Zhang, P-Z., Bai, Q-F., 1991. Synoptic climatology of cyclogenesis over East Asia. *Mon. Weather*
531 *Rev.* 119, 1407-1418.
- 532 Christensen, J.H., Krishna Kumar, K., Aldrian, E., An, S.-I., Cavalcanti, I.F.A., de Castro, M., Dong, W., Goswami, P.,
533 Hall, A., Kanyanga, J.K., Kitoh, A., Kossin, J., Lau, N.-C., Renwick, J., Stephenson, D.B., Xie, S.-P., Zhou, T., 2013.
534 Climate Phenomena and their Relevance for Future Regional Climate Change. In: *Climate Change 2013: The Physical*
535 *Science Basis. Contribution of Working Group I to the Fifth Assessment Report of the Intergovernmental Panel on*
536 *Climate Change* [Stocker, T.F., Qin, D., Plattner, G.-K., Tignor, M., Allen, S.K., Boschung, J., Nauels, A., Xia, Y., Bex,
537 V. Midgley, P.M. (eds.)]. Cambridge University Press, Cambridge, United Kingdom and New York, NY, USA.
- 538 Craine, J.M., Nippert, J.B., Elmore, A.J., Skibbe, A.M., Hutchinson, S.L., Brunzell, N.A., 2012, Timing of climate
539 variability and grassland productivity. *109, P. Natl. Acad. Sci, USA.* 3401-3405.
- 540 Crowther, T.W., Todd-Brown, K.E.O., Rowe, C.W., Wieder, W.R., Carey, J. C., Machmuller, M.B., Snoek, B.L., Fang, S.,
541 Zhou, G., Allison, S.D., Blair, J.M., Bridgman, S.D., Burton, A.J., Carrillo, Y., Reich, P.B., Clark, J.S., Classen, A.T.,
542 Dijkstra, F.A., Elberling, B., Emmett, B.A., Estiarte, M., Frey, S.D., Guo, J., Harte, J., Jiang, L., Johnson, B.R., Kröel-
543 Dulay, G., Larsen, K.S., Laudon, H., Lavalley, J.M., Luo, Y., Lupascu, M., Ma, L.N., Marhan, S., Michelsen, A.,
544 Mohan, J., Niu, S., Pendall, E., Peñuelas, J., Pfeifer-Meister, L., Poll, C., Reinsch, S., Reynolds, L.L., Schmidt, I.K.,
545 Sistla, S., Sokol, N.W., Templer, P.H., Treseder, K.K., Welker, J.M., Bradford, M.A., 2016. Quantifying global soil
546 carbon losses in response to warming. *Nature* 540, 104-108.
- 547 Davi, N.K., Jacoby, G.C., Curtis, A.E., Nachin, B., 2006. Extension of drought records for central Asia using tree rings:
548 West central Mongolia. *J. Clim.*, 19, 288-299.
- 549 Davi, N., Jacoby, G., D'Arrigo, R., Baatarbileg, N., Li, J., Curtis, A., 2009. A tree-ring based drought index reconstruction
550 for far western Mongolia: 1565–2004. *Int. J. Climatol.* 29, 1508-1514.

- 551 Davi, N., Jacoby, G., Fang, K., Li, J., D'Arrigo, R., Baatarbileg, N., Robinson, D., 2010. Reconstructing drought
552 variability for Mongolia based on a large-scale tree ring network: 1520-1993. *J. Geophys. Res.* 115, D22103.
- 553 Endo, N., Kadota, T., Matsumoto, J., Ailikun, B., Yasunari, T., 2006. Climatology and Trends in Summer Precipitation
554 Characteristics in Mongolia for the Period 1960–98. *J. Meteorol. Soc. Jpn.* 84, 543-551.
- 555 Frolova, N.L., Belyakova, P.A., Grigoriev, V.Y., Sazonov, A.A., Zotov, L.V., Jarsjö, J., 2017. Runoff fluctuations in the
556 Selenga River Basin. *Reg. Environ. Change*. doi:10.1007/s10113-017-1199-0.
- 557 Forkel, M., Thonicke, K., Beer, C., Cramer, W., Bartalev, S., Schmullius, C., 2012. Extreme fire events are related to
558 previous-year surface moisture conditions in permafrost-underlain larch forests of Siberia. *Environ. Res. Lett.* 7,
559 044021.
- 560 Hansen, M.C., Potapov, P.V., Moore, R., Hancher, M., Turubanova, S.A., Tyukavina, A., Thau, D., Stehman, S.V., Goetz,
561 S.J., Loveland, T.R., Kommareddy, A., Egorov, A., Chini, L., Justice, C.O., Townshend, J.R.G., 2013. High-resolution
562 global maps of 21st-century forest cover change. *Science* 342, 850-853.
- 563 Haywood, A.M., Dowsett, H.J., Dolan, A.M., 2016. Integrating geological archives and climate models for the mid-
564 Pliocene warm period. *Nat. Commun.* 7, 10646.
- 565 Hijioka, Y., Lin, E., Pereira, J.J., Corlett, R.T., Cui, X., Insarov, G.E., Lasco, R.D., Lindgren, E., Surjan, A., 2014. Asia, in:
566 Barros, V.R., Field, C.B., Dokken, D.J., Mastrandrea, M.D., Mach, K.J., Bilir, T.E., Chatterjee, M., Ebi, K.L., Estrada,
567 Y.O., Genova, R.C., Girma, B., Kissel, E.S., Levy, A.N., MacCracken, S., Mastrandrea, P.R., White, L.L. (Eds.),
568 Climate Change 2014: Impacts, Adaptation, and Vulnerability. Part B: Regional Aspects. Contribution of Working
569 Group II to the Fifth Assessment Report of the Intergovernmental Panel on Climate Change. Cambridge University
570 Press, Cambridge, United Kingdom and New York, NY, USA, pp. 1327-1370.
- 571 Hohmann R., Kipfer R., Peeters F., Piepke G., Imboden D.M., Shimaraev M.N., 1997. Deep-water renewal in Lake Baikal.
572 *Limnol. Oceanogr.* 42, 841-855.
- 573 IPCC, 2012. Managing the Risks of Extreme Events and Disasters to Advance Climate Change Adaptation. A Special
574 Report of Working Groups I and II of the Intergovernmental Panel on Climate Change, in: Field, C.B., Barros, V.,
575 Stocker, T.F., Qin, D., Dokken, D.J., Ebi, K.L., Mastrandrea, M.D., Mach, K.J., Plattner, G.-K., Allen, S.K., Tignor, M.,
576 Midgley, P.M. (Eds.), Cambridge University Press, Cambridge, UK, and New York, NY, USA, 582 pp.
- 577 Iwao, K., Ttakahashi, M., 2006. Interannual change in summertime precipitation over northeast Asia. *Geophys. Res. Lett.*
578 33, L16703.
- 579 Iwao, K., Ttakahashi, M., 2008. A Precipitation seesaw mode between Northeast Asia and Siberia in Summer caused by
580 Rossby waves over the Eurasian continent. *J. Clim.* 21, 2401-2419.
- 581 Karthe, D., Chalov, S., Borchardt, D., 2015. Water resources and their management in central Asia in the early twenty first
582 century: status, challenges and future prospects. *Environ. Earth. Sci.* 73, 487-499.
- 583 Kavvada, A., Ruiz-Barradas, A., Nigam, S., 2013, AMO's structure and climate footprint in observations and IPCC AR5
584 climate simulations. *Clim. Dyn.* 41, 1345-1364.
- 585 Kipfer, R., AeschbachHertig, W., Hofer, M., Hohmann, R., Imboden, D.M., Baur, H., Golubev, V., Klerkx, J., 1996.
586 Bottomwater formation due to hydrothermal activity in Frolikha Bay, Lake Baikal, eastern Siberia. *Geochim.*
587 *Cosmochim. Acta.* 60, 961-971.
- 588 Kostrova, S.S., Meyer, H., Chaplignin, B., Kossler, A., Bezrukova, E.V., Tarasov, P.E., 2013., Holocene oxygen isotope
589 record of diatoms from Lake Kotokel (southern Siberia, Russia) and its palaeoclimatic implications. *Quatern Int.* 290-
590 291, 21-34.
- 591 Kurita, N., Yoshida N., Inoue, G., Chayanova, E.A, 2004., Modern isotope climatology of Russia: A first assessment. *J*
592 *Geophys Res.* 109, D03102, doi:10.1029/2003JD003404.
- 593 Leng, M.J., Barker, P., 2006. A review of the oxygen isotope composition of lacustrine diatom silica for palaeoclimate
594 reconstruction. *Earth Sci. Rev.* 75, 5-27.
- 595 Leng, M.J., Sloane, H.J., 2008. Combined oxygen and silicon isotope analysis of biogenic silica. *Journal of Quaternary*
596 *Science* 23, 313-319.
- 597 Li, C., Zhang, C., Luo, G., Chen, X., Maisupova, B., Madaminov, A.A., Han, Q., Djenbaev, B.M., 2015. Carbon stock and
598 its responses to climate change in Central Asia. *Glob. Change. Biol.* 21, 1951-1967.
- 599 Liu, Y.Y., Evans, J.P., McCabe, M.F., de Jeu, R.A.M., van Dijk, A.I.J.M., Dolman, A.J., Saizen, I., 2013. Changing Climate
600 and Overgrazing Are Decimating Mongolian Steppes. *PLOS One* 8, e57599.
- 601 Lu, Y., Zhuang, Q., Zhou, G., Sirin, A., Melillo, J., Kicklighter, D., 2009. Possible decline of the carbon sink in the
602 Mongolian Plateau during the 21st century. *Environ. Res. Lett.* 4, 045023.
- 603 Lydolph, P.E., 1977. Eastern Siberia. In: *Climates of the Soviet Union. World Survey of Climatology*, vol. 7. Elsevier, pp.
604 91-115.

- 605 Mackay, A., Flower, R., Kuzmina, A., Granina, L., Rose, N., Appleby, P., Boyle, J., and Battarbee, R., 1998., Diatom
606 succession trends in recent sediments from Lake Baikal and their relation to atmospheric pollution and to climate
607 change, *Philos. T. Roy. Soc. B*, 353, 1011-1055.
- 608 Mackay, A.W., Karabanov, E., Khursevich, G., Leng, M., Morley, D.W., Panizzo, V.N., Sloane, H.J., Williams, D., 2008.
609 Reconstructing hydrological variability in Lake Baikal during MIS 11: an application of oxygen isotope analysis of
610 diatom silica. *J Quaternary Sci.*, 23, 365-374.
- 611 Mackay, A.W., Swann, G.E.A., Brewer, T., Leng, M.J., Morley, D.W., Piotrowska, N., Rioual, P., White, D., 2011. A
612 reassessment of late glacial-Holocene diatom oxygen isotope records from Lake Baikal using a mass balance approach.
613 *J Quaternary Sci.* 26, 627-634
- 614 Mackay, A.W., Swann, G.E.A., Fagel, N., Fietz, S., Leng, M.J., Morley, D., Rioual, P., Tarasov, P. 2013., Hydrological
615 instability during the Last Interglacial in central Asia: a new diatom oxygen isotope record from Lake Baikal.
616 *Quaternary Sci. Rev.* 66, 45-54.
- 617 Mackay, A.W., Seddon, A.W.R., Leng, M.J., Heumann, G., Morley, D.W., Piotrowska, N., Rioual, P., Roberts, S., Swann,
618 G.E.A., 2017. Holocene carbon dynamics at the forest - steppe ecotone of southern Siberia. *Glob. Change Biol.* 23,
619 1942-1960.
- 620 Moore, G.W.K., Halfar, J., Majeed, H., Adey, W., Kronz, A., 2017, Amplification of the Atlantic Multidecadal Oscillation
621 associated with the onset of the industrial-era warming. *Sci Rep-UK*, 7:40861.
- 622 Moore, M.V., Hampton, S.E., Izmet'eva, L.R., Silow, E.A., Peshkova, E.V., Pavlov, B.K., 2009. Climate Change and the
623 World's "Sacred Sea"-Lake Baikal, Siberia. *BioScience* 49, 405-417.
- 624 Morley, D.W., Leng, M.J., Mackay, A.W., Sloane, H.J., 2005. Late Glacial and Holocene atmospheric circulation change in
625 the Lake Baikal region documented by oxygen isotopes from diatom biogenic silica. *Global Planet. Change* 46, 221-
626 233.
- 627 PAGES Hydro2k Consortium, 2017., Comparing proxy and model estimates of hydroclimate variability and change over
628 the Common Era, *Clim Past*, 13, 1851-1900,
- 629 Panizzo V.N., Swann, G.E.A., Mackay, A.W., Vologina, E., Alleman, L., Andre, L., Pashley, V.H., Horstwood, M.S.A.,
630 2017., Constraining modern day silicon cycling in Lake Baikal. *Global Biogeochem Cy.* 31, 556-574.
- 631 Pederson, N., Jacoby, G., D'Arrigo, R., Cook, E., Buckley, B., Dugarjav, C., Mijiddorj, R., 2001. Hydrometeorological
632 reconstructions for north-eastern Mongolia derived from tree rings: AD 1651–1995, *J. Clim.* 14, 872-881.
- 633 Popovskaya, G.I., 2000. Ecological monitoring of phytoplankton in Lake Baikal. *Aquatic Ecosystem Health and*
634 *Management* 3, 215-225.
- 635 Randerson, J.T., Liu, H., Flanner, M.G., Chambers, S.D., Jin, Y., Hess, P.G., Pfister, G., Mack, M.C., Treseder, K.K.,
636 Welp, L.R., Chapin, F.S., Harden, J.W., Goulden, M.L., Lyons, E., Neff, J.C., Schuur, E.A.G., Zender, C.S., 2006.
637 The Impact of Boreal Forest Fire on Climate Warming. *Science* 314, 1130-1132.
- 638 Ravens, T.M., Kocsis, O., Wüest, A., Granin, N., 2000. Small-scale turbulence and vertical mixing in Lake Baikal. *Limnol.*
639 *Oceanogr.* 45, 159-173.
- 640 Rioual, P., Mackay, A.W., 2005., A diatom record of centennial resolution for the the Kazantsevo Interglacial stage in Lake
641 Baikal (Siberia). *Global Planet Change* 46, 199-219.
- 642 Romanovsky, V.E., Drozdov, D.S., Oberman, N.G., Malkova, G.V., Kholodov, A.L., Marchenko, S.S., Moskalenko, N.G.,
643 Sergeev, D.O., Ukraintseva, N.G., Abramov, A.A., Gilichinsky, D.A., Vasiliev, A.A., 2010., Thermal state of permafrost
644 in Russia. *Permafrost Periglac.* 21, 136-155.
- 645 Ryves, D.B., Jewson, D.H., Sturm, M., Battarbee, R.W., Flower, R.J., Mackay, A.W., Granin, N. G., 2003., Quantitative
646 and qualitative relationships between planktonic diatom communities and diatom assemblages in sedimenting material
647 and surface sediments in Lake Baikal, Siberia. *Limnol. Oceanogr.*, 48, 1643–1661.
- 648 Sato, T., Kimura, F., Kitoh, A., 2007. Projection of global warming onto regional precipitation over Mongolia using a
649 regional climate model. *J. Hydrol.* 333, 144-154.
- 650 Schuur, E.A.G., McGuire, A.D., Schädel, C., Grosse, G., Harden, J.W., Hayes, D.J., Hugelius, G., Koven, C.D., Kuhry, P.,
651 Lawrence, D.M., Lawrence, S.M., Olefeldt, D., Romanovsky, V.E., Schaefer, K., Turetsky, M.R., Treat, C.C., Vonk,
652 J.E., 2015. Climate change and the permafrost carbon feedback. *Nature* 520, 171-179.
- 653 Seal, R.R., Shanks, W.C., 1998. Oxygen and hydrogen isotope systematics of Lake Baikal, Siberia: implications for
654 palaeoclimate studies. *Limnol. Oceanogr.* 43, 1251-1261.
- 655 Selvam, B.P., Lapierre, J-F., Guillemette, F., Voigt, C., Lamprecht, R.E., Biasi, C., Christensen, T.R., Martikainen, P.J.,
656 Berggren, M., 2017. Degradation potentials of dissolved organic carbon (DOC) from thawed permafrost peat. *Sci Rep-*
657 *UK* 7, 45811.
- 658 Seim, A., Schultz, J., Leland, C., Davi, N., Byambasuren, O., Liang, E., Wang, X., Beck, C., Linderholm, H.W., Pederson,

- 659 N., 2017., Synoptic-scale circulation patterns during summer derived from tree rings in mid-latitude Asia. *Clim Dyn.*
660 49, 1917-1931.
- 661 Settele, J., Scholes, R., Betts, R., Bunn, S., Leadley, P., Nepstad, D., Overpeck, J.T., Taboada, M.A., 2014, Terrestrial and
662 inland water systems, in Field, C.B., Barros, V.R., Dokken, D.J., Mach, K.J., Mastrandrea, M.D., Bilir, T.E., Chatterjee,
663 M., Ebi K.L., Estrada, Y.O., Genova, R.C., Girma, B., Kissel, E.S., Levy, A.N., MacCracken, S., Mastrandrea, P.R.,
664 White, L.L. (Eds.), *Climate Change 2014: Impacts, Adaptation, and Vulnerability. Part A: Global and Sectoral Aspects.*
665 *Contribution of Working Group II to the Fifth Assessment Report of the Intergovernmental Panel on Climate Change.*
666 Cambridge University Press, Cambridge, United Kingdom and New York, NY, USA, pp. 271-359.
- 667 Shahgedanova, M., 2002. Climate at present and in the historical past. In: Shahgedanova, M. (Ed.), *The Physical*
668 *Geography of Northern Eurasia.* OUP, Oxford, pp. 70-102.
- 669 Sharkuu N., 1998. Trends in permafrost development in the Selenge River basin, Mongolia. *Collection Nordicana*, 55,
670 979-985.
- 671 Shimaraev M.N., Granin N.G., 1991. Temperature stratification and the mechanisms of convection in Lake Baikal. *Dokl.*
672 *Akad. Nauk.* 321, 381-385.
- 673 Shimaraev M.N., Domysheva V.M., 2004. Climate and long-term silica dynamics in Lake Baikal. *Russ. Geol. Geophys.*
674 45, 310-316.
- 675 Shimaraev M.N., Granin N.G., Zhdanov A.A., 1993. Deep ventilation of Lake Baikal waters due to spring thermal bars.
676 *Limnol. Oceanogr.* 38, 1068-1072.
- 677 Shimaraev, M.N., Verbolov, V.I., Granin, N.G., Sherstyankin, P.P., 1994. Physical Limnology of Lake Baikal. A review. In:
678 Shimaraev, M.N., Okuda, S. (Eds.), BICER Publishers, Irkutsk. 81 pp.
- 679 Shimaraev, M.N., Troitskaya, E.S., Blinov, V.V., Ivanov, V.G., Gnatovskii, R.Yu., 2012. Upwellings in Lake Baikal. *Dokl.*
680 *Earth Sc.* 442, 272-276.
- 681 Solovieva, N, Tarasov P.E., MacDonald, G., 2005. Quantitative reconstruction of Holocene climate from the Chuna Lake
682 pollen record, Kola Peninsula, northwest Russia. *Holocene* 15, 141-148.
- 683 Sturm M., Vologina E.G., Vorob'eva S.S., 2016. Holocene and Late Glacial sedimentation near steep slopes in southern
684 Lake Baikal. *J. Limnology.* 75, 24-35.
- 685 Sugita, M., Yoshizawa, S., Byambakhuu, I., 2015, Limiting factors for nomadic pastoralism in Mongolian steppe: a
686 hydrologic perspective. *J. Hydrol.* 524, 455-467.
- 687 Sun, C., Li, J., Zhao, S., 2015. Remote influence of Atlantic multidecadal variability on Siberian warm season
688 precipitation. *Sci. Rep-UK.* 5, 16853.
- 689 Swann, G.E.A., Pike, J., Snelling, A.M., Leng, M.J., Williams, M.C., 2013. Seasonally resolved diatom $\delta^{18}\text{O}$ records from
690 the west Antarctic Peninsula over the last deglaciation. *Earth Planet. Sci. Lett.* 364, 12-23.
- 691 Tarasov, P., Bezrukova, E., Karabanov, E., Nakagawa, T., Wagner, M., Kulagina, N., Letunova, P., Abzaeva, A.,
692 Granoszewski, W., Riedel, F., 2007. Vegetation and climate dynamics during the Holocene and Eemian interglacials
693 derived from Lake Baikal pollen records. *Palaeogeogr. Palaeoclimatol.* 252, 440-457.
- 694 Tarasov, P.E., Bezrukova, E.V., Krivonogov, S.K., 2009. Late Glacial and Holocene changes in vegetation cover and
695 climate in southern Siberia derived from a 15 kyr long pollen record from Lake Kotokel. *Clim. Past.* 5, 285-295.
- 696 Tautenhahn, S.T., Lichstein, J.W., Jung, M., Kattge, J., Bohlman, S.A., Heilmeyer, H., Prokushkin, A., Kahl, A., Wirth, C.,
697 2016. Dispersal limitation drives successional pathways in Central Siberian forests under current and intensified fire
698 regimes. *Glob. Change Biol.* 22, 2178-2197.
- 699 Tchebakova, N.M., Parfenova, E., Soja, A.J., 2009. The effects of climate, permafrost and fire on vegetation change in
700 Siberia in a changing climate. *Environ. Res. Lett.* 4 045013.
- 701 Tchebakova, N.M., Parfenova, E.I., Korets, M.A., Conard, S.G., 2016. Potential change in forest types and stand heights in
702 central Siberia in a warming climate. *Environ. Res. Lett.* 11, 035016.
- 703 Törnqvist, R., Jarsjö, J., Pietroń, J., Bring, A., Rogberg, P., Asokan, S.M., Destouni, G., 2014. Evolution of the hydro-
704 climate system in the Lake Baikal basin. *J. Hydrol.* 519, 1953-1962.
- 705 Troitskaya, E., Blinov, V., Ivanov, V., Zhdanov, A., Gnatovsky, R., Sutyryna, E., Shimaraev, M., 2015. Cyclonic circulation
706 and upwelling in Lake Baikal. *Aquat. Sci.* 77, 171-182.
- 707 Tsimitri, C., Rockel, B., Wüest, A., Budnev, N.M., Sturm, M., Schmid, M., 2015. Drivers of deep-water renewal events
708 observed over 13 years in the South Basin of Lake Baikal. *J. Geophys. Res. Oceans*, 120, 1508-1526.
- 709 Vologina, E.G., Kashik, S.A., Sturm, M., Vorob'eva, S.S., Lomonosova, T.K., Kalashnikova, I.A., Khramtsova, T.I.,
710 Toshchakov, S.Yu., 2007. Results of research into Holocene sediments of the South and Central basins of Lake Baikal
711 (BDP-97 and short cores). *Russ. Geol. Geophys.* 48, 312-323.

- 712 Weiss, R.F., Carmak, E.C., Koropalov, V.M., 1991. Deep-water renewal and biological production in Lake Baikal. *Nature*
713 349, 665-669.
- 714 Wang, W., Feng, Z., 2013. Holocene moisture evolution across the Mongolian Plateau and its surrounding areas: A
715 synthesis of climatic records. *Earth-Sci. Rev.* 122, 38-57.
- 716 Wu, X, Liu, H, Guo, D, Anenkhonov, O.A., Badmaeva, N.K., Sanddanov, D.V., 2012. Growth Decline Linked to Warming-
717 Induced Water Limitation in Hemi-Boreal Forests. *PLoS ONE* 7, e42619. doi:10.1371/journal.pone.0042619.
- 718 Zhao, L., Wu, Q., Marchenko, S.S., Sharkuu, N., 2010. Thermal state of permafrost and active layer in central Asia during
719 the International Polar Year. *Permafrost Periglac.* 21, 198-207.

720

721 Acknowledgements

722 This work was supported by Natural Environment Research Council grants NE/J00829X/1, NE/J010227/1, and
723 NE/J007765/1). The authors are indebted to the assistance of Nikolaj M. Budnev (Irkutsk State University), the
724 captain and crew of the Geolog research boat together with Dmitry Gladkochub (IEC) in facilitating and
725 organizing all Russian fieldwork. A final thanks is owed to Neil Rose and Handong Yang who carried out the
726 ²¹⁰Pb dating at the UCL Environmental Radiometric Facility and to the anonymous reviewers as well as guest
727 editor (Oliver Heiri) who's comments significantly improved the manuscript.

728

729 Supplementary Information

730 Supplementary Table 1: Diatom oxygen isotope ($\delta^{18}\text{O}_{\text{diatom}}$) and reconstructed precipitation for south basin
731 sediment cores BAIK13-1C, BAIK13-4F and BAIK13-7A used in the composite $\delta^{18}\text{O}_{\text{diatom}}$ record.

732

733 Supplementary Table 2: Holocene $\delta^{18}\text{O}_{\text{diatom}}$ from Vydrino Shoulder (Lake Baikal) (Mackay et al., 2011) and
734 reconstructed precipitation.